1.3. COMPARISON OF RADIOSONDE AND RUC MODEL MEAN RADIATING TEMPERATURE OF THE ATMOSPHERE

Zlatko R. Vukovic* and J. Walter Strapp
Cloud Physics and Severe Weather Research Section,
Environment Canada, Toronto, Canada

1. INTRODUCTION

In order to acquire measurements of precipitable water vapor (PWV) and precipitable liquid water (PLW) from a dual-frequency ground based microwave radiometer, an accurate statistical retrieval algorithm is required to convert raw brightness temperaratures into PWP and PLW. These algorithms include a set of input parameters whose values vary according to location, season, and weather conditions (Westwater 1978). One of these input parameters, the mean radiating temperature of the atmosphere (T_{mr}), can be estimated using different techniques (Chiswell et al. 1994).

Over the last decade the resolution and accuracy of numerical weather prediction (NWP) models has continually improved. The accessibility of the model output has also significantly improved, to the point that the operational use of T_{mr} obtained from NWP models should now be considered, as a replacement for the current method of producing T_{mr} from seasonal or monthly averaged climatological values from radiosonde measurements.

The main objective of this study is to examine the use of the 'real-time' NWP T_{mr} in microwave radiometer statistical retrievals rather than seasonal averaged climatological T_{mr} values from radiosonde measurements, , and to assess differences in accuracy.

2. ACURACY OF THE STATISCAL RETRIEVAL

The Radiometrics WVR-1000 microwave radiometer measures sky brightness temperature T_b at two frequencies: 23.8 GHz ("vapor" channel) and 31.4 GHz ("liquid" channel). Because T_b is not a linear function of PWV and PLW, the linear quantity opacity τ, is derived.

$$\tau = \ln\left(\frac{T_{mr} - 2.75}{T_{mr} - T_b}\right). \quad (1)$$

In (1), T_b is a measured quantity and T_{mr} is estimated.

From (1) we find that the error in opacity ($\delta\tau$) is proportional to the errors in T_{mr} and T_a:

$$\frac{\delta\tau}{\tau} \approx \frac{\delta T_{mr}}{T_{mr}} + \frac{\delta T_a}{T_a} \,. \quad (2)$$

This indicates that an improvement in the estimation of T_{mr} leads to a better estimation of opacity, and consequently more accurate PWL and PLW retrievals.

3. DATA AND METHODOLOGY

One full year (2003) of radiosonde and the Rapid Update Cycle (RUC) model data, (Benjamin et al. 2004), were analyzed for Maniwaki, Ontario radiosonde site location for two standard times: 0h and 12h UTC.

The RUC model used has 20 km horizontal resolution (RUC20) and 50 computation levels. Only a reduced amount of RUC model data was available during the summer period.

T_{mr} for 23.8 and 31.4 GHz were derived from both the radiosonde and RUC model vertical profiles, using the same algorithm used by the Radiometric Corporation for the WVR-1100 retrievals (Fredrick Solheim private correspondence).

* Zlatko R. Vukovic, Environment Canada, 4905 Dufferin Street, Toronto, ON, Canada, M3H 5T4; e-mail: zlatko.vukovic@ec.gc.ca

The data from four RUC forecast times (3h, 6h, 9h, and 12h) were used in the comparison with the radiosonde data.

4. DATA ANALYSIS AND COMPARISONS

The radiosonde and RUC time series of T_{mr} are shown in Figure 1. Plots of T_{mr} for 23.8 and 31.4 GHz are shown on the left and right sides of the figure respectively. The forecast time increases from the top to the bottom.

From Figure 1 it can be seen that the RUC T_{mr} was consistently higher than the corresponding radiosonde values. The differences became greater in warmer periods. A possible explanation for this could be increasing differences in model predictions and observed profiles of relative humidity with increasing convective dynamics in the warmer periods (Benjamin et al. 2004). Further analysis would be required to validate this suggestion.

The scatter diagrams of the radiosonde-RUC T_{mr} values (Fig. 2) show a linear correlation. In Table 1 the corresponding correlation coefficients range from .92 to 0.97 (Table 1). The correlation was the strongest for the 3 h forecast, for the 31.8 GHz frequency, and become weaker as the forecast times increased. The slopes of best-fit lines were about 1.3 and 1.2, for 23.8 and 31.4 GHz, respectively. Therefore the corresponding rms was quite high, at ~13 and 8 ^{o}K respectively, which leads to unacceptable errors in the operational estimate of T_{mr} using the RUC model.

Since a strong correlation exists between the radiosonde and RUC T_{mr}, it is possible to make a simple adjustment to the RUC T_{mr} based on the radiosonde-RUC regressions. This new RUC T_{mr} data set is referred to as the corrected RUC T_{mr} ($T_{mr}^{\sim}$):

$$T_{mr}^{\sim} = \frac{T_{mr}}{a} - \frac{b}{a}, \qquad (3)$$

where a is the slope and b is the intercept of the linear correlation between radiosonde and the RUC T_{mr}.

From the time series and the scatter diagrams of the corrected RUC model $T_{mr}^{\sim}$ (Figs. 3 and 4.) it can be seen that, as expected, the corrected set of RUC T_{mr} fits well with the radiosonde T_{mr} and the correlation coefficients were in the same range as for uncorrected T_{mr}. More importantly the rms had much lower values, in the range of 2.7 to 4.2 ^{o}K, when compared to the pre-corrected values.

Table 2 shows the rms, relative rms, the average T_{mr} of the atmosphere, and the total number of points for the following five periods: a full year (2003), December - February, March – May, Jun – August, and September – November, for computed for both frequencies from radiosonde and RUC data .

For the radiosonde, rms was calculated relative to the mean value of radiosonde T_{mr}, while for the RUC rms was calculated with respect to the corresponding radiosonde T_{mr} value. In other words, radiosonde rms values quantify the dispersion of T_{mr} from the mean value for the selected period, while the RUC rms quantifies the difference between radiosonde and RUC T_{mr}.

The rms differences between the radiosonde and RUC T_{mr} values were in the range of 2.5 to 5.2 ^{o}K (0.9-2.0 %), which was much better than the radiosonde differences of 3.5 to 8.0 ^{o}K (1.3-3.0 %) from it's averaged T_{mr} values, for the same seasonal periods.

	23.8 GHz					31.4 GHz					
	rms (^{o}K)	rel. rms (%)	***a***	***b*** (^{o}K)	Corr Coef	rms (^{o}K)	rel. rms (%)	***a***	***b*** (^{o}K)	Corr Coef	N
RUC-03h	12.6	4.8	1.34	-78	0.96	7.6	2.8	1.21	-50	0.97	494
RUC-06h	13.1	4.9	1.34	-79	0.94	8.2	3.1	1.21	-50	0.95	490
RUC-09h	12.9	4.9	1.34	-79	0.93	8.3	3.1	1.21	-50	0.94	489
RUC-12h	12.3	4.7	1.34	-80	0.92	7.9	3.0	1.21	-50	0.93	490

Table 1. Summary of the root-mean-square (rms), relative rms, slope a, intercept b, and correlation coefficient of a linear correlation between RUC and Maniwaki radiosonde mean radiating temperature T_{mr}, and the number of radiosonde - RUC points for two frequencies, 23.8 and 31.4 GHz, for 3, 6, 9, and 12 h RUC forecast durations.

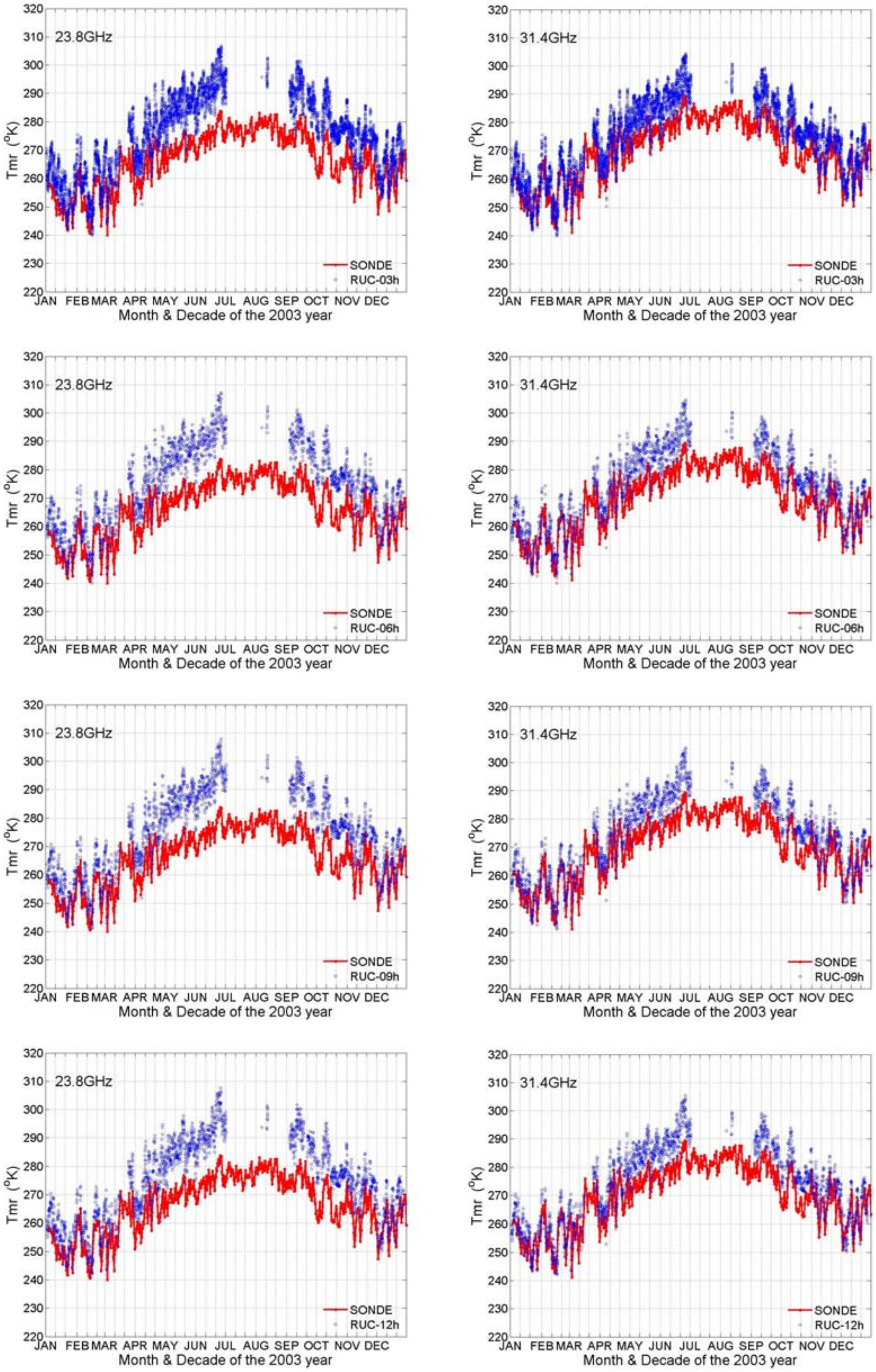

Fig. 1. Time history of T_{mr} for 23.8 GHz (left) and 31.4 GHz (right) for 3, 6, 9, and 12h forecast durations (from top to bottom).

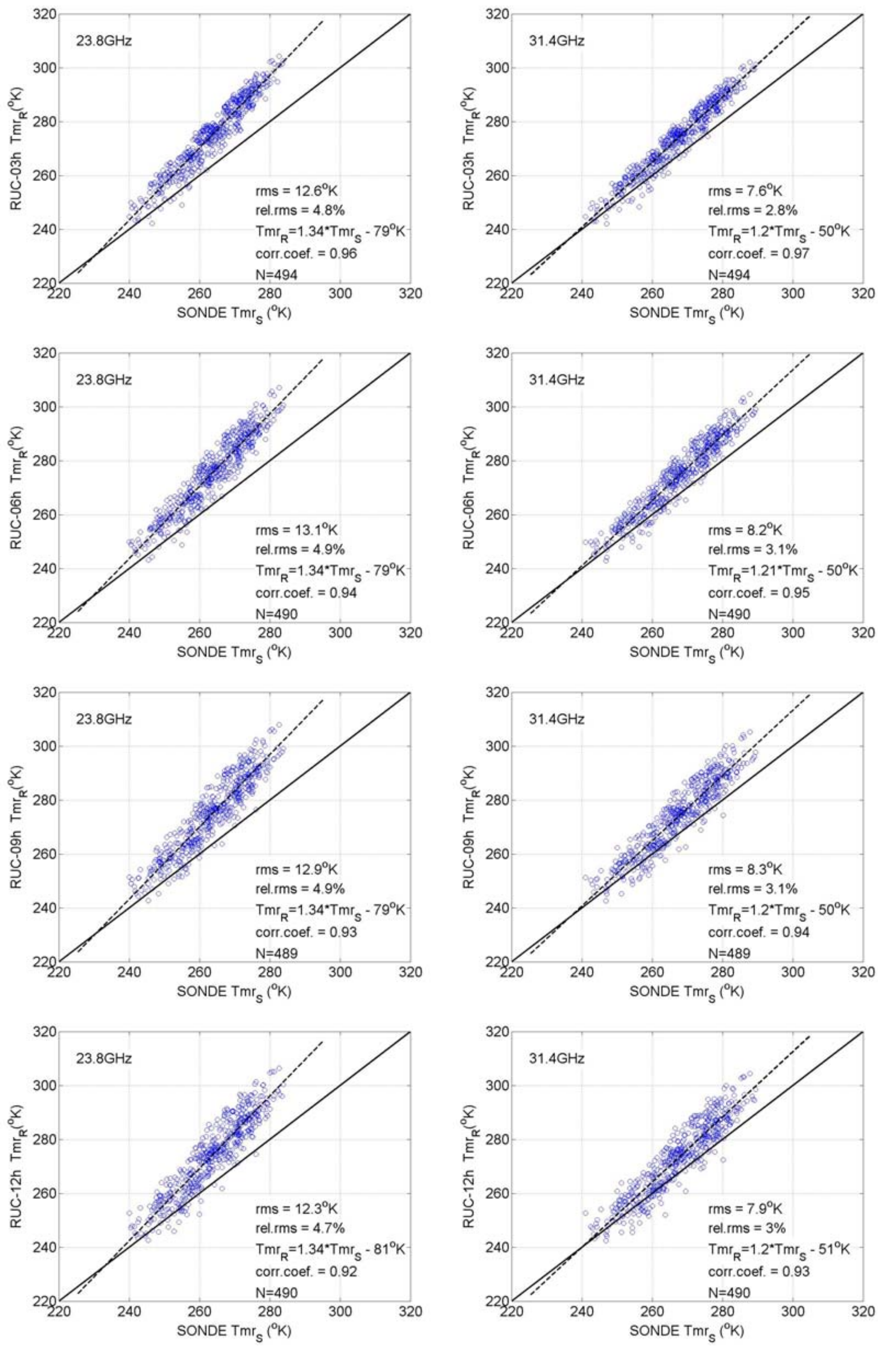

Fig. 2. Scatter diagrams of T_{mr} for 23.8 GHz (left) and 31.4 GHz (right) for 3, 6, 9, and 12h forecast durations (from top to bottom).

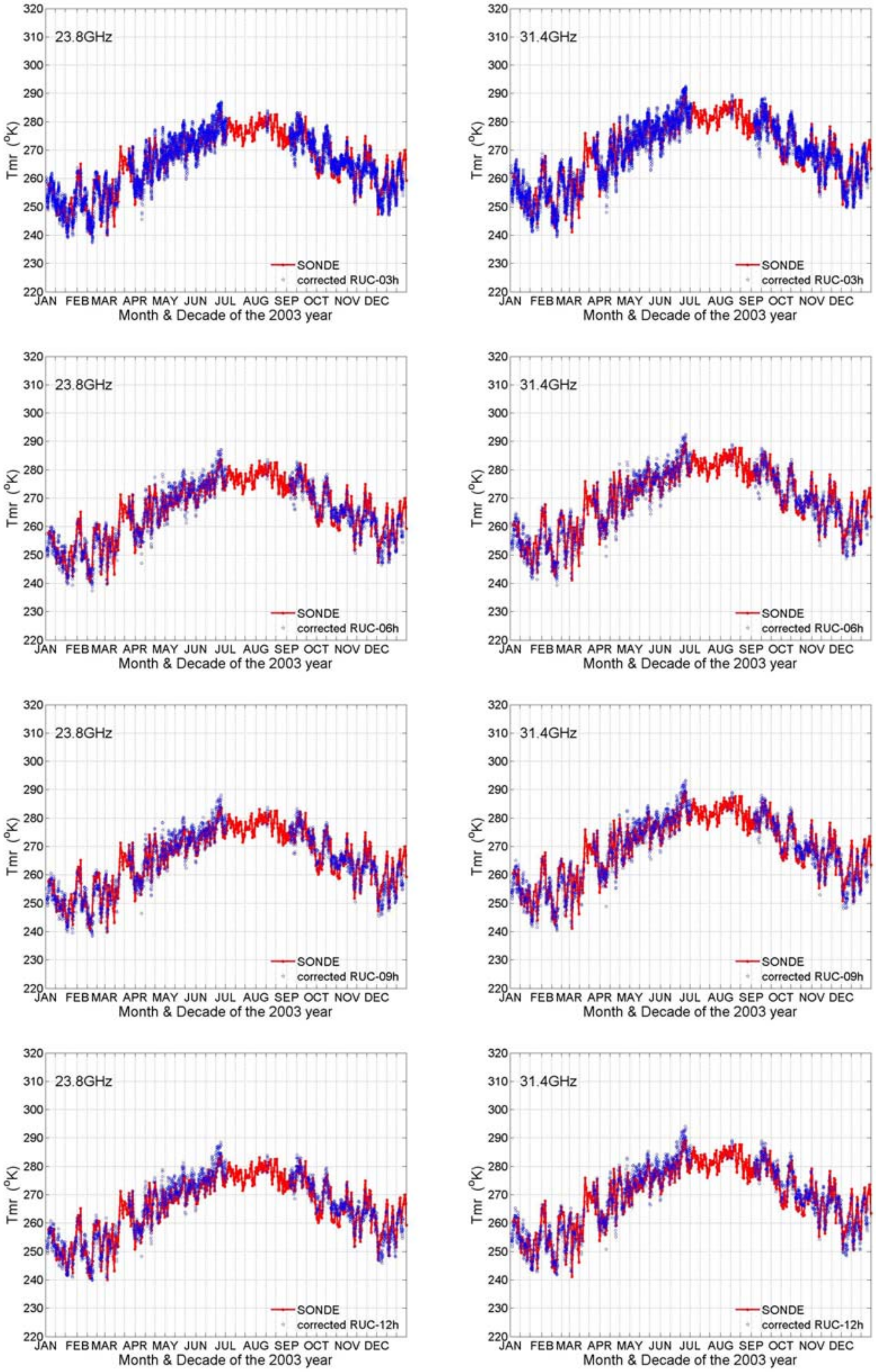

Fig. 3. Time history of corrected T_{mr} for 23.8 GHz (left) and 31.4 GHz (right) for 3, 6, 9, and 12h forecast durations (from top to bottom).

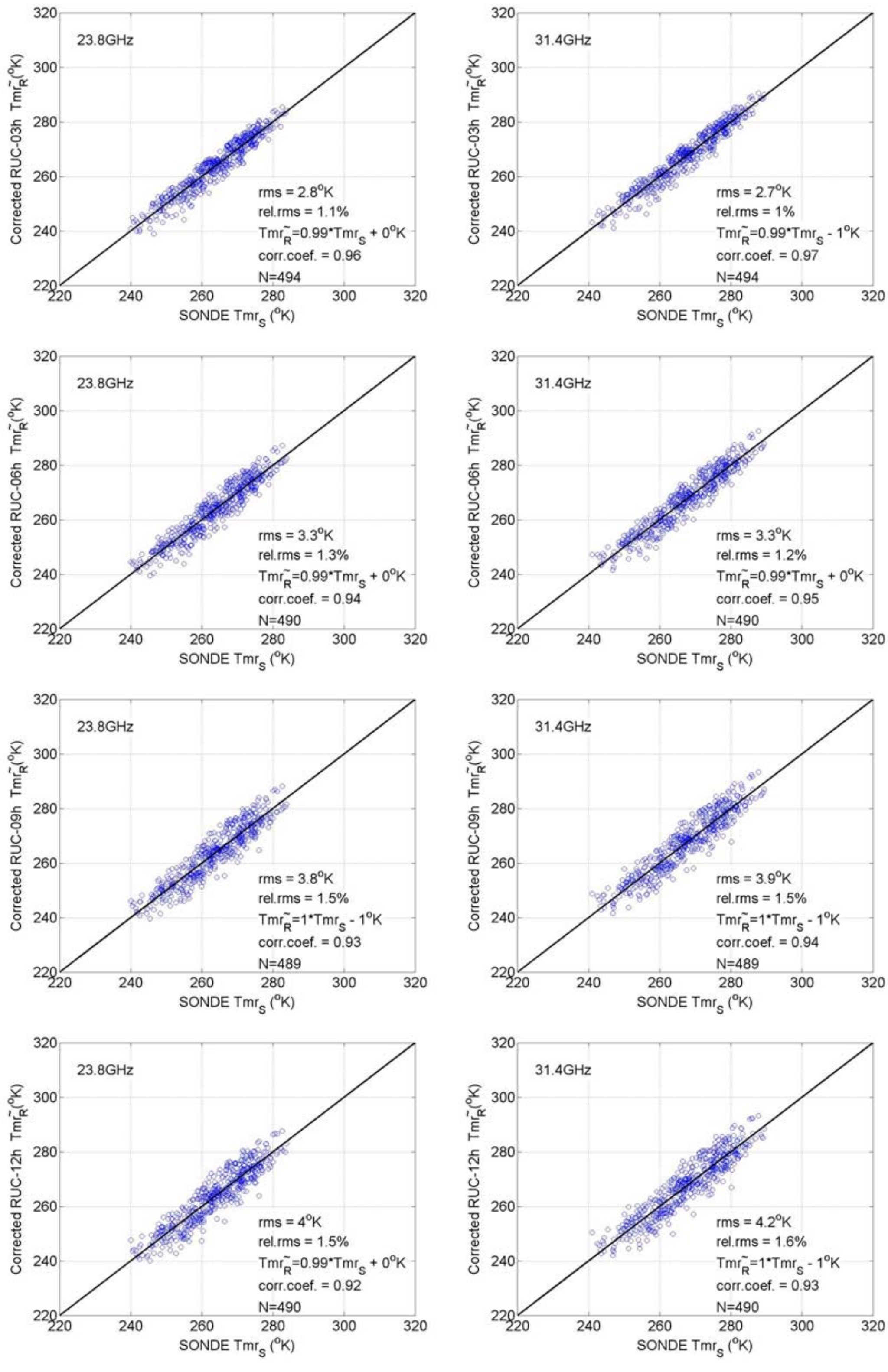

Fig. 4. Scatter diagrams of corrected T_{mr} for 23.8 GHz (left) and 31.4 GHz (right) for 3, 6, 9, and 12h forecast durations (from top to bottom).

			Period				
			2003	Dec Feb	Mar May	Jun Aug	Sep Nov
23.8 GHz	rms (°K)	Sonde	10.0	6.8	7.3	3.5	6.4
		RUC03	3.6	3.4	2.6	2.5	4.8
		RUC06	4.0	3.6	3.4	3.4	5.0
		RUC09	4.5	3.9	4.2	4.2	5.2
		RUC12	4.5	3.9	4.5	4.2	5.1
	rel. rms (%)	Sonde	3.7	2.7	2.8	1.3	2.4
		RUC03	1.4	1.3	1.0	0.9	1.8
		RUC06	1.5	1.4	1.3	1.2	1.9
		RUC09	1.7	1.5	1.6	1.5	2.0
		RUC12	1.7	1.5	1.7	1.5	1.9
	T_{mr} (°K)	Sonde	266	254	265	277	268
		RUC03	264	253	266	277	267
		RUC06	264	252	266	277	268
		RUC09	264	252	266	277	268
		RUC12	264	252	266	277	268
	N	Sonde	691	156	169	182	184
		RUC03	495	141	143	57	154
		RUC06	491	141	143	55	152
		RUC09	490	141	142	55	152
		RUC12	491	141	142	55	153
31.4 GHz	rms (°K)	Sonde	10.8	7.2	8.0	3.7	6.8
		RUC03	3.7	3.2	2.4	2.4	5.2
		RUC06	4.1	3.5	3.4	3.4	5.3
		RUC09	4.6	3.9	4.3	4.3	5.5
		RUC12	4.8	4.0	4.8	4.6	5.4
	rel. rms (%)	Sonde	4.0	2.8	3.0	1.3	2.5
		RUC03	1.4	1.3	0.9	0.8	1.9
		RUC06	1.5	1.4	1.3	1.2	2.0
		RUC09	1.7	1.5	1.6	1.5	2.0
		RUC12	1.8	1.6	1.8	1.6	2.0
	T_{mr} (°K)	Sonde	270	257	269	281	272
		RUC03	268	256	270	282	271
		RUC06	268	255	270	282	272
		RUC09	268	255	270	282	272
		RUC12	268	255	269	282	272
	N	Sonde	691	156	169	182	184
		RUC03	495	141	143	57	154
		RUC06	491	141	143	55	152
		RUC09	490	141	142	55	152
		RUC12	491	141	142	55	153

Table 2. Summary of the rms, relative rms, averaged T_{mr}, and total number of points N for the five periods (2003 full year, and 4 seasons: Dec-Feb, Mar-May, Jun-Aug, Sep-Nov) for 23.8 and 31.4 GHz frequencies.

Table 3 shows the variation in the relative number of hours (per season) for five classes (0-5; 6-10; 11-15; 16-20; >20°K) of absolute difference between the average seasonal radiosonde T_{mr} and the RUC model 3 h forecast T_{mr} (ΔT_{mr}) for the 31.4 GHz channel at the Maniwaki location (WMW). Also shown is the amount of relative error (r.err.) decrease if the RUC T_{mr} is used instead of the seasonally averaged radiosonde T_{mr}. The total number of hours per season for each ΔT_{mr} class is also shown (N).

The graphical presentation of relative frequency (r.rf.) of the relative errors (r.err.) of Table 3, is shown in Fig.5.

ΔT_{mr} (°K)		Dec-Feb	Mar-May	Jun-Aug	Sep-Nov
0-5	r.fr.(%)	54.6	39.2	72.1	52.7
	r.err.(%)	1.9	1.9	1.8	1.8
	N	1059	725	511	961
6-10	r.fr.(%)	29.9	38.1	22.4	34.3
	r.err.(%)	3.9	3.7	3.6	3.7
	N	580	705	159	626
11-15	r.fr.(%)	14.4	18.7	5.5	11.8
	r.err.(%)	5.8	5.6	5.3	5.5
	N	280	346	39	215
16-20	r.fr.(%)	1.0	2.9	0.0	1.2
	r.err.(%)	7.8	7.4	7.1	7.4
	N	20	53	0	21
>20	r.fr.(%)	0.0	1.0	0.0	0.0
	r.err.(%)	0.0	9.3	0.0	0.0
	N	0	19	0	0

Table 3. Summary of the changing relative frequency (r.fr.), relative error (r.err. = ΔT_{mr} / avT_{mr}), and the total number of RUC output hours during the season (N), versus the absolute differences between the average seasonal radiosonde 31.4 GHz T_{mr} and the RUC model 3 h forecast 31.4 GHz T_{mr} (ΔT_{mr}). Data are shown for the four seasons (Dec-Feb, Mar-May, Jun-Aug, Sep-Nov) for Maniwaki (WMW).

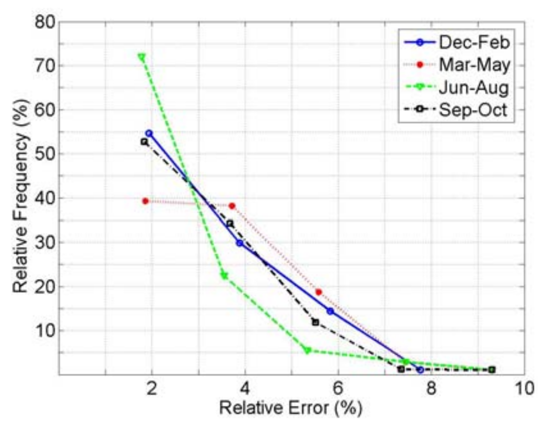

Fig. 5. The relative frequency of the relative error if it used seasonal averaged T_{mr} instead of the RUC 3 h forecast T_{mr} for the 31.4 GHz frequency.

The data presented in Table 3 and Figure 5 show that if the adjusted RUC T_{mr} is used instead of a constant average seasonal T_{mr} from historical radiosonde data, in about ¼ of the instances (from a cumulative relative frequency) the relative error decreased by more than 5%.

The Jun-Aug period was incomplete and thus the Relative Frequency to Relative Error dependency is slightly different than that of the other seasons.

4. SUMMARY AND CONCLUSIONS

From a one year data set of Maniwaki radiosonde and RUC data, the mean radiating temperature (T_{mr}) values for 23.8 and 31.4 GHz were calculated. The data were linearly correlated, but with a slope in a range of 1.2 – 1.3 (RUC being the dependant variable), and with rms values in a range of 8 – 13 ^{o}K.

After an adjustment based on this regression was applied to the RUC T_{mr}, the new data set naturally had a 1:1 linear correlation. For the five periods including the full year of 2003, Dec-Feb, Mar-May, Jun-Aug, and Sep-Nov, the rms difference between the radiometer and the adjusted RUC T_{mr} values was in the range of 2.5 to 5.2 ^{o}K, which was much better than the , 3.5 to 10.0 ^{o}K radiosonde rms difference from it's averaged T_{mr} values for the same periods.

When using seasonal averaged radiosonde-derived values of T_{mr} in PWV and PLW retrievals, greater error is generated than if the corrected forecasted RUC T_{mr} values were used.

Three main points regarding to use of T_{mr} in radiometric retrievals can be concluded from this study:

a) The T_{mr} calculated from the RUC model forecasts can be successfully substituted for T_{mr} derived from historical radiosonde data. In this study the linear correlation increased from 0.92 for 12 h forecast (23.8 GHz) to 0.97 for a 3 h forecast (31.4 GHz).

b) The use of RUC model T_{mr} can often result in improved accuracy of T_{mr} relative to historical radiosonde-derived values. In this study, it was shown that the improvement was > 5% in about 25% of the cases. Maximum improvement was 8%.

c) The use of the RUC model forecast data may also reduce errors in regions where radiosonde historical data are not available.

Acknowledgments:
The author would like to thank Fredrick Solheim from Radiometrics Co. for providing his T_{mr} algorithm, and Mark Couture for his very useful suggestions.

REFERENCES

Benjamin, S. G., D. Dévényi, S. S. Weygandt, K. J. Brundage, J. M. Brown, G. A. Grell, D. Kim, B. E. Schwartz, T. G. Smirnova, T. L. Smith and G. S. Manikin, 2004: An Hourly Assimilation–Forecast Cycle: The RUC. *Monthly Weather Review*: Vol. *132*, No. **2**, pp. 495–518.

Chiswell S. R., S. Businger, M. Bevis, F. Solheim, C. Rocken and R. Ware, 1994: Improved Retrieval of Integrated Water Vapor from Water Vapor Radiometer Measurements Using Numerical Weather Prediction Models. *Journal of Atmospheric and Oceanic Technology*: Vol. *11*, No. **5**, pp. 1253–1261.

Westwater, E. R., 1978: The accuracy of water vapor and cloud liquid determinations by dual-frequency ground-based microwave radiometry. *Radio Sci*., **13**, 677-685.